Stabilization of Kelvin-Helmholtz instabilities in 3D linearized Euler equations using a non-dissipative discontinuous Galerkin method

Serge Piperno, Marc Bernacki

European Conference on Computational Fluid Dynamics
ECCOMAS CFD 2006
P. Wesseling, E. Oñate and J. Périaux (Eds)

STABILIZATION OF KELVIN-HELMHOLTZ INSTABILITIES IN 3D LINEARIZED EULER EQUATIONS USING A NON-DISSIPATIVE DISCONTINUOUS GALERKIN METHOD

Marc Bernacki and Serge Piperno

Cermics, projet Caiman
Ecole des Ponts (ParisTech) et INRIA
Cité Descartes, Chanps-sur-Marne, 77455 Marne-la-Valle cedex 2, France
e-mail: serge.piperno@cermics.enpc.fr, marc.bernacki@ensmp.fr,
web page: http://cermics.enpc.fr/~piper/

Key words: aeroacoustics; acoustic energy; linearized Euler equations; non-uniform steady-state flow; Discontinuous Galerkin method; time domain; energy-conservation.

Abstract. *We present in this paper a time-domain Discontinuous Galerkin dissipation-free method for the transient solution of the three-dimensional linearized Euler equations around a steady-state solution. In the general context of a non-uniform supporting flow, we prove, using the well-known symmetrization of Euler equations, that some aeroacoustic energy satisfies a balance equation with source term at the continuous level, and that our numerical framework satisfies an equivalent balance equation at the discrete level and is genuinely dissipation-free. Moreover, there exists a correction term in aeroacoustic variables such that the aeroacoustic energy is exactly preserved, and therefore the stability of the scheme can be proved. This leads to a new filtering of Kelvin-Helmholtz instabilities. In the case of* $\mathbb{P}_1$ *Lagrange basis functions and tetrahedral unstructured meshes, a parallel implementation of the method has been developed, based on message passing and mesh partitioning. Three-dimensional numerical results confirm the theoretical properties of the method. They include test-cases where Kelvin-Helmholtz instabilities appear and can be eliminated by addition of the source term.*

1 INTRODUCTION

Aeroacoustics is a domain where numerical simulation meets great expansion. The minimization of acoustic pollutions by aircrafts at landing and take off, or more generally by aerospace and terrestrial vehicles, is now an industrial concern, related to more and more severe norms. Different approaches coexist under the Computational Aeroacoustics activity. The most widely used methods belong to classical Computational Fluid Dynamics and consist in solving partial differential equations for the fluid, without distinction

between the supporting (possibly steady-state) flow and acoustic perturbations[1]. The equations modeling the fluid can be Euler or Navier-Stokes equations, possibly including extended models like turbulence, LES techniques, etc[2]. One particular difficulty of these approaches is the difference in magnitude between the flow and acoustic perturbations, then requiring very accurate – and CPU-consuming – numerical methods.

An alternative has developed recently with approaches consisting in separating the determination of the supporting steady-state flow and in modeling the generation of noise (for example by providing equivalent acoustic sources), from the propagation of acoustic perturbations[3, 4, 5]. For this problem, linearized Euler equations around the supporting flow are to be solved and provide a good description of the propagation of aeroacoustic perturbations in a smoothly varying heterogeneous and anisotropic medium. This is not exactly the case of more simple models based on Lighthill analogy[6] or of the third-order equation of Lilley[7] (a clear description can be found in a more recent reference[8]). The noise source modeled or derived from the steady-state flow are then dealt with as acoustic source terms in the linearized Euler equations.

The work presented here is devoted to the numerical solution of linearized Euler equations around steady-state discretized flows, obtained using a given Euler solver. The supporting flow considered is always smooth and subsonic, it can be uniform or fully non-uniform. Since we intend to consider complex geometries in three space dimensions, we consider unstructured tetrahedral space discretizations. In this context, we propose a time domain Discontinuous Galerkin dissipation-free method based on $\mathbb{P}_1$ Lagrange elements on tetrahedra. The method is derived from similar methods developed for three-dimensional time-domain Maxwell equations[9]. We use an element-centered formulation with centered numerical fluxes and an explicit leap-frog time scheme. This kind of method provides a dissipation-free approximation of propagation equations and allows for the accurate estimation of aeroacoustic energy variation, which is not possible with numerical methods (finite volumes, discontinuous Galerkin, spectral elements) based on upwind numerical fluxes.

More precisely, the main results of this paper concern both the linearized Euler equations at the continuous level, and the numerical method we propose. They can be summed up the following way:

1. for a uniform supporting flow, at the continuous level (i.e. before space discretization), some quadratic energy verifies a balance equation without source term. This means energy is conserved (up to boundaries);

2. in this "uniform supporting flow" case, we are able to prove that our Discontinuous Galerkin method (with leap-frog time-scheme and centered fluxes) introduces no dissipation even on unstructured simplicial meshes (some discrete energy is exactly conserved, or simply non-increasing when absorbing boundary conditions are used); therefore we claim that we "control energy variations in the uniform case";

3. accordingly, for a non-uniform supporting flow, at the continuous level (i.e. before space discretization), we use the well-known symmetrization of nonlinear Euler equations [10] to derive an aeroacoustic energy which verifies some balance equation with source term. Because of this unsigned source term, aeroacoustic waves can be damped or excited by the supporting flow. It is responsible for example for Kelvin-Helmholtz instabilities. These instabilities are due to the model (linearized Euler equations), not to the numerical method;

4. in the "non uniform supporting flow" case, we are able to prove that, using an adapted version of the same Discontinuous Galerkin method on unstructured simplicial meshes, some "discrete" energy balance equation with source term is also verified. We claim our method is still non-dissipative. The good point is that we are able to reproduce these instabilities. The bad point is that we cannot damp them artificially (like methods based on upwind fluxes, which damp instabilities, in an uncontrolled way though);

5. we show finally that there exists a discrete source term such that energy is exactly conserved and the stability of the scheme can be proved. Therefore the non-dissipative DGTD method provides an accurate tool for controlling phenomena like Kelvin-Helmholtz instabilities.

2 LINEARIZATION OF EULER EQUATIONS

We consider here equations for the propagation of acoustic waves through a steady smooth inviscid flow. Therefore, we linearize the three-dimensional Euler equations around a given steady flow and only take into account first-order perturbation terms. For a perfect inviscid gas, Euler equations read:

$$\partial_t \begin{pmatrix} \rho \\ \rho u \\ \rho v \\ \rho w \\ e \end{pmatrix} + \partial_x \begin{pmatrix} \rho u \\ \rho u^2 + p \\ \rho uv \\ \rho uw \\ (e+p)u \end{pmatrix} + \partial_y \begin{pmatrix} \rho v \\ \rho uv \\ \rho v^2 + p \\ \rho vw \\ (e+p)v \end{pmatrix} + \partial_z \begin{pmatrix} \rho w \\ \rho uw \\ \rho vw \\ \rho w^2 + p \\ (e+p)w \end{pmatrix} = 0, \qquad (1)$$

where ρ, $\vec{v} = {}^t(u, v, w)$, e and p denote respectively the density, the velocity, the volumic total energy and the pressure, given by the perfect gas law $p = (\gamma - 1)(e - \frac{1}{2}\rho\|\vec{v}\|^2)$, where γ is a fixed constant ($\gamma > 1$).

When the steady supporting flow is uniform, the equations obtained by linearizing the Euler equations are simple, in the sense that they naturally involve symmetric matrices and lead to a Friedrich's system (if the intuitive conservative variables are used). This symmetry also lead naturally energy conservation properties. However, things are more complex when the steady supporting flow is not uniform. In that case, the steady flow is defined by smoothly varying physical quantities $(\rho_0, \vec{v}_0, p_0)$. Linearizing straightforwardly

Euler equations (1) yields:

$$\partial_t \vec{\mathbf{W}} + \partial_x \left(\mathbb{A}_x^0 \vec{\mathbf{W}} \right) + \partial_y \left(\mathbb{A}_y^0 \vec{\mathbf{W}} \right) + \partial_z \left(\mathbb{A}_z^0 \vec{\mathbf{W}} \right) = 0, \tag{2}$$

where $\vec{\mathbf{W}}$ now denotes the perturbations of conservative variables (i.e. $\vec{\mathbf{W}}^T = (\delta\rho,\ \rho_0\delta\vec{v} + \vec{v}_0\delta\rho,\ \delta p/(\gamma-1) + \rho_0\vec{v}_0.\delta\vec{v} + \|\vec{v}_0\|^2\delta\rho/2)$) and the space-varying matrices $\mathbb{A}_x^0$, $\mathbb{A}_y^0$, and $\mathbb{A}_z^0$ are given in function of $\tilde{\gamma} = \gamma - 1$, $\alpha_0 = c_0^2/\tilde{\gamma} + \|\vec{v}_0\|^2/2$, $\beta_0 = (\gamma-2)\|V_0\|^2/2 - c_0^2/\tilde{\gamma}$, and the canonical basis $(\vec{e}_x, \vec{e}_y, \vec{e}_z)$ of $\mathbb{R}^3$ by

$$\mathbb{A}_s^0 = \begin{pmatrix} 0 & {}^t\vec{e}_s & 0 \\ \frac{\tilde{\gamma}}{2}\|\vec{v}_0\|^2\vec{e}_s - (\vec{v}_0.\vec{e}_s)\vec{v}_0 & (\vec{v}_0.\vec{e}_s)\mathbb{I}_3 - \tilde{\gamma}\vec{e}_s\,{}^t\vec{v}_0 + \vec{v}_0\,{}^t\vec{e}_s & \tilde{\gamma}\vec{e}_s \\ \beta_0(\vec{v}_0.\vec{e}_s) & \alpha_0\,{}^t\vec{e}_s - \tilde{\gamma}(\vec{v}_0.\vec{e}_s)\,{}^t\vec{v}_0 & \gamma(\vec{v}_0.\vec{e}_s) \end{pmatrix},\ s \in \{x,y,z\}. \tag{3}$$

In this equation, the matrices $\mathbb{A}_x^0$, $\mathbb{A}_y^0$, and $\mathbb{A}_z^0$ are not symmetric anymore, and it is very difficult to deduce any aeroacoustic energy balance equation. Therefore, we consider other acoustic variables, derived from the quite classical symmetrization of Euler equations. Assuming the flow is smooth enough, the change of variables $(\rho, \rho\vec{v}, e) \rightarrow (-\frac{e\tilde{\gamma}}{p} + \gamma + 1 - \ln\left(\frac{p}{\rho^\gamma}\right), \frac{\rho\tilde{\gamma}}{p}\vec{v}, -\frac{\rho\tilde{\gamma}}{p})$ transforms Euler equations (1) into a symmetric system of conservation laws (i.e. Jacobians of fluxes are symmetric matrices). Accordingly, the linearization of these symmetrized Euler equations leads to more complex aeroacoustic equations for perturbations of the new variables, which can be written as

$$\mathbb{A}_0^0 \partial_t \vec{\mathbf{V}} + \partial_x \left(\tilde{\mathbb{A}}_x^0 \vec{\mathbf{V}} \right) + \partial_y \left(\tilde{\mathbb{A}}_y^0 \vec{\mathbf{V}} \right) + \partial_z \left(\tilde{\mathbb{A}}_z^0 \vec{\mathbf{V}} \right) = 0, \tag{4}$$

where $\vec{\mathbf{V}}$ is given in function of variables $\vec{\mathbf{W}}$ by $\vec{\mathbf{V}} = {\mathbb{A}_0^0}^{-1}\vec{\mathbf{W}}$ and

$$\mathbb{A}_0^0 = \frac{\rho_0}{\tilde{\gamma}} \begin{pmatrix} 1 & {}^t\vec{v}_0 & \alpha_0 - c_0^2/\gamma \\ \vec{v}_0 & \frac{c_0^2}{\gamma}\mathbb{I}_3 + \vec{v}_0\,{}^t\vec{v}_0 & \alpha_0\vec{v}_0 \\ \alpha_0 - c_0^2/\gamma & \alpha_0\,{}^t\vec{v}_0 & \alpha_0^2 - c_0^4/(\gamma\tilde{\gamma}) \end{pmatrix};\ \tilde{\mathbb{A}}_s^0 = \mathbb{A}_s^0\mathbb{A}_0^0,\ s \in \{x,y,z\}. \tag{5}$$

$\mathbb{A}_0^0$ clearly is symmetric and it can be proved that it is definite positive (and then not singular). Eq. 4 can also be obtained simply by replacing $\vec{\mathbf{W}}$ by $\mathbb{A}_0^0\vec{\mathbf{V}}$ in Eq. 2 (and by noting that $\partial_t\mathbb{A}_0^0 = 0$). Finally, the reader can also check that the symmetric matrices $\tilde{\mathbb{A}}_s$ ($s \in \{x,y,z\}$) are given by

$$\tilde{\mathbb{A}}_s^0 = (\vec{v}_0.\vec{e}_s)\ \mathbb{A}_0^0 + \frac{p_0}{\tilde{\gamma}} \begin{pmatrix} 0 & {}^t\vec{e}_s & (\vec{v}_0.\vec{e}_s) \\ \vec{e}_s & \vec{e}_s\,{}^t\vec{v}_0 + \vec{v}_0\,{}^t\vec{e}_s & (\vec{v}_0.\vec{e}_s)\vec{v}_0 + \alpha_0\vec{e}_s \\ (\vec{v}_0.\vec{e}_s) & (\vec{v}_0.\vec{e}_s)\,{}^t\vec{v}_0 + \alpha_0\,{}^t\vec{e}_s & 2\alpha_0(\vec{v}_0.\vec{e}_s) \end{pmatrix}.$$

Then, the volumic aeroacoustic energy $\mathcal{E}$ defined by $\mathcal{E} = \frac{1}{2}\,{}^t\vec{\mathbf{W}}{\mathbb{A}_0^0}^{-1}\vec{\mathbf{W}} \equiv \frac{1}{2}\,{}^t\vec{\mathbf{V}}\mathbb{A}_0^0\vec{\mathbf{V}}$ verifies the following balance equation with source term:

$$\partial_t\mathcal{E} + \mathrm{div}\vec{\mathcal{F}} = \mathcal{S},\ \text{with}\ \begin{cases} \mathcal{F}_s = {}^t\vec{\mathbf{V}}\tilde{\mathbb{A}}_s^0\vec{\mathbf{V}},\ s \in \{x,y,z\}. \\ \mathcal{S} = -\frac{1}{2}\,{}^t\vec{\mathbf{V}}\left[\partial_x(\tilde{\mathbb{A}}_x^0) + \partial_y(\tilde{\mathbb{A}}_y^0) + \partial_z(\tilde{\mathbb{A}}_z^0)\right]\vec{\mathbf{V}}. \end{cases} \tag{6}$$

Thus the aeroacoustic energy is not conserved and the variations in the steady flow considered can damp or amplify aeroacoustic waves, unless the source term vanishes (which is the case for a uniform flow for example). In the sequel, we shall mainly discretize the conservative form (2), but we shall need the equivalent symmetric form (4) for discussions concerning energy conservation and stability.

3 A DISCONTINUOUS GALERKIN TIME-DOMAIN METHOD

Discontinuous Galerkin methods have been widely used with success for the numerical simulation of acoustic or electromagnetic wave propagation in the time domain[9, 11]. The very same type of methods can be used for the problems considered here, i.e. the propagation of aeroacoustic waves through a non-uniform flow[12]. In this section, we present the DGTD method we use for the model equations (2). We recall the numerical properties of the space discretization. Then we introduce the leap-frog time scheme and give some details on properties related to energy conservation and stability.

In the whole paper, we assume we dispose of a partition of a polyhedral domain Ω (whose boundary $\partial\Omega$ is the union of physical boundaries of objects $\partial\Omega^{\text{phys}}$ and of the far field artificial boundary $\partial\Omega^{\infty}$). Ω is partitioned into a finite number of polyhedra (each one having a finite number of faces). For each polyhedron $\mathcal{T}_i$, called "control volume" or "cell", V_i denotes its volume. We call face between two control volumes their intersection, whenever it is a polyhedral surface. The union of all faces $\mathcal{F}$ is partitioned into internal faces $\mathcal{F}^{\text{int}} = \mathcal{F}/\partial\Omega$, physical faces $\mathcal{F}^{\text{phys}} = \mathcal{F} \bigcap \partial\Omega^{\text{phys}}$ and absorbing faces $\mathcal{F}^{\text{abs}} = \mathcal{F} \bigcap \partial\Omega^{\infty}$. For each internal face $a_{ik} = \mathcal{T}_i \bigcap \mathcal{T}_k$, we denote by S_{ik} the measure of a_{ik} and by $\vec{n}_{ik}$ the unitary normal, oriented from $\mathcal{T}_i$ towards $\mathcal{T}_k$. The same definitions are extended to boundary faces, the index k corresponding to a fictitious cell outside the domain. Finally, we denote by $\mathcal{V}_i$ the set of indices of the control volumes neighboring a given control volume $\mathcal{T}_i$ (having a face in common). We also define the perimeter P_i of $\mathcal{T}_i$ by $P_i = \sum_{k\in\mathcal{V}_i} S_{ik}$. We recall the following geometrical property for all control volumes: $\sum_{k\in\mathcal{V}_i} S_{ik}\vec{n}_{ik} = 0$.

Following the general principle of discontinuous Galerkin finite element methods, the unknown field inside each control volume is seeked for as a linear combination of local basis vector fields $\vec{\varphi}_{ij},\ 1 \leq j \leq d_i$ (generating the local space $\mathcal{P}_i$) and the approximate field is allowed to be fully discontinuous across element boundaries. Thus, a numerical flux function has to be defined to approximate fluxes at control volumes interfaces, where the approximate solution is discontinuous.

This context is quite general. Actual implementations of the method have been considered only on tetrahedral meshes, where control volumes are the tetrahedra themselves. We shall only consider constant ($\mathbb{P}_0$) or linear ($\mathbb{P}_1$) approximations inside tetrahedra.

3.1 Time and space discretizations

We only consider here the most general case of aeroacoustic wave propagation in a non-uniform steady flow. Also, in order to limit the amount of computations, we restrict our study to piecewise constant matrices $\mathbb{A}_s^0$ ($s \in \{x, y, z\}$) given in Eq. (3). For each control volume $\mathcal{T}_i$, for $s \in \{x, y, z\}$, we denote by $\mathbb{A}_s^i$ an approximate for the average value of $\mathbb{A}_s^0$ over $\mathcal{T}_i$. Dot-multiplying Eq. (2) by any given vector field $\vec{\varphi}$, integrating over $\mathcal{T}_i$ and integrating by parts yields

$$\int_{\mathcal{T}_i} \vec{\varphi} \cdot \frac{\partial \vec{\mathbf{W}}}{\partial t} = \int_{\mathcal{T}_i} \left(\sum_{s\in\{x,y,z\}} {}^t\partial_s \vec{\varphi}\, \mathbb{A}_s^0 \right) \vec{\mathbf{W}} - \int_{\partial\mathcal{T}_i} \vec{\varphi} \cdot \left(\sum_{s\in\{x,y,z\}} n_s \mathbb{A}_s^0 \vec{\mathbf{W}} \right). \tag{7}$$

Inside volume integrals over $\mathcal{T}_i$, we replace the field $\vec{\mathbf{W}}$ by the approximate field $\vec{\mathbf{W}}_i$ and the matrices $\mathbb{A}_s^0$ by their respective average values $\mathbb{A}_s^i$. For boundary integrals over $\partial\mathcal{T}_i$, $\vec{\mathbf{W}}$ is discontinuous, and we define totally centered numerical fluxes, i.e.:

$$\left\{ \begin{array}{l} \forall i, \forall k \in \mathcal{V}_i, \left[(n_{ik_x}\mathbb{A}_x^0 + n_{ik_y}\mathbb{A}_y^0 + n_{ik_z}\mathbb{A}_z^0)\vec{\mathbf{W}} \right]_{|a_{ik}} \simeq \frac{1}{2}\left(\mathbb{P}_{ik}^i \vec{\mathbf{W}}_i + \mathbb{P}_{ik}^k \vec{\mathbf{W}}_k \right), \\ \text{with} \quad \mathbb{P}_{ik}^i = n_{ik_x}\mathbb{A}_x^i + n_{ik_y}\mathbb{A}_y^i + n_{ik_z}\mathbb{A}_z^i, \qquad \mathbb{P}_{ik}^k = n_{ik_x}\mathbb{A}_x^k + n_{ik_y}\mathbb{A}_y^k + n_{ik_z}\mathbb{A}_z^k. \end{array} \right. \tag{8}$$

Concerning the time discretization, we use a three-level leap-frog scheme. The unknowns $\vec{\mathbf{W}}_i$ are approximated at integer time-stations $t^n = n\Delta t$. Assuming we dispose of $\vec{\mathbf{W}}_i^{n-1}$ and $\vec{\mathbf{W}}_i^n$, the unknowns $\vec{\mathbf{W}}_i^{n+1}$ are seeked for in $\mathcal{P}_i$ such that, $\forall \vec{\varphi} \in \mathcal{P}_i$,

$$\int_{\mathcal{T}_i} \vec{\varphi} \cdot \frac{\vec{\mathbf{W}}_i^{n+1} - \vec{\mathbf{W}}_i^{n-1}}{2\Delta t} = \int_{\mathcal{T}_i} \sum_{s\in\{x,y,z\}} {}^t\partial_s \vec{\varphi}\, \mathbb{A}_s^i \vec{\mathbf{W}}_i^n - \sum_{k\in\mathcal{V}_i} \int_{a_{ik}} \vec{\varphi} \cdot \frac{\mathbb{P}_{ik}^i \vec{\mathbf{W}}_i^n + \mathbb{P}_{ik}^k \vec{\mathbf{W}}_k^n}{2}. \tag{9}$$

Again, the time scheme above is almost explicit. Each time step only requires the inversion of local symmetric positive definite matrices of size $(d_i \times d_i)$. In the particular case where $\mathcal{P}_i$ is a complete linear ($\mathbb{P}_1$) representation, these 20×20 matrices are indeed made of 5 4×4 diagonal blocks (which are equal to the classical $\mathbb{P}_1$ mass matrix).

3.2 Boundary conditions

Boundary conditions are dealt with in a weak sense. For the physical boundary, we consider only a slip condition, which is set on both the steady flow and the acoustic perturbations. This means that we assume that for any slip boundary face a_{ik} belonging to the control volume $\mathcal{T}_i$, the steady solution of Euler equations verifies a slip condition at the discrete level, *i.e.* $\vec{n}_{ik} \cdot \vec{v}_i^0 = 0$. For the acoustic perturbations, we use a mirror fictitious state $\vec{\mathbf{W}}_k$ in the computation of the boundary flux given in Eq. (9). We take $\delta\rho_k = \delta\rho_i$, $\delta p_k = \delta p_i$, and $\delta\vec{v}_k = \delta\vec{v}_i - 2(\vec{n}_{ik} \cdot \vec{v}_i)\vec{n}_{ik}$ (which implies $(\delta\vec{v}_k - \delta\vec{v}_i) \times \vec{n}_{ik} = 0$ and $\delta\vec{v}_k.\vec{n}_{ik} = -\delta\vec{v}_i.\vec{n}_{ik}$).

For an absorbing boundary face a_{ik}, upwinding is used to select outgoing waves only. Before discretization in time, classical upwinding leads to a boundary flux $\mathbb{F}_{ik}$ given by $\mathbb{F}_{ik} = (\mathbb{P}^i_{ik})^+ \vec{\mathbf{W}}_i$, where for any diagonalizable matrix $\mathbb{Q} = \mathbb{S}^{-1}\mathbb{D}\mathbb{S}$ with $\mathbb{D}$ diagonal, $\mathbb{Q}^+ = (\mathbb{Q}+|\mathbb{Q}|)/2$ and terms of the diagonal matrix $|\mathbb{D}|$ are the moduli of the eigenvalues. This general idea leads to $\mathbb{P}^k_{ik}\vec{\mathbf{W}}_k = |\mathbb{P}^i_{ik}|\vec{\mathbf{W}}_i$. However, for this intuitive numerical flux, it is very difficult to prove that the resulting time-scheme is stable and that energy is actually sent in the exterior domain. We then consider the numerical flux based on the following fictitious state: $\mathbb{P}^k_{ik}\vec{\mathbf{W}}^n_k = \sqrt{\mathbb{A}}^i_0 \left|\sqrt{\mathbb{A}}^{i\,-1}_0 \mathbb{P}^i_{ik} \sqrt{\mathbb{A}}^i_0\right| \sqrt{\mathbb{A}}^{i\,-1}_0 \frac{\vec{\mathbf{W}}^{n-1}_i + \vec{\mathbf{W}}^{n+1}_i}{2}$, where $\sqrt{\mathbb{A}}^i_0$ is the positive square root of the symmetric definite positive matrix $\mathbb{A}^i_0$. Indeed, this expression derives from the intuitive upwind flux for the symmetrized equations (4). It leads to time-scheme which is locally implicit near absorbing boundaries (i.e. independent linear systems are to be solved inside elements having at least one absorbing face, at each time step). It leads to a globally second-order time-accurate scheme. A less accurate explicit version is also available[12]. It takes the form $\mathbb{P}^k_{ik}\vec{\mathbf{W}}^n_k = \sqrt{\mathbb{A}}^i_0 \left|\sqrt{\mathbb{A}}^{i\,-1}_0 \mathbb{P}^i_{ik} \sqrt{\mathbb{A}}^i_0\right| \sqrt{\mathbb{A}}^{i\,-1}_0 \vec{\mathbf{W}}^{n-1}_i$.

3.3 Energy balance and stability

In order to investigate stability, we define a discrete aeroacoustic energy $\mathbb{F}^n$ by:

$$\begin{aligned}\mathbb{F}^n &= \frac{1}{2}\sum_i \int_{\mathcal{T}_i} {}^t\vec{\mathbf{W}}^n_i \mathbb{A}^{i\,-1}_0 \vec{\mathbf{W}}^n_i + {}^t\vec{\mathbf{W}}^{n+1}_i \mathbb{A}^{i\,-1}_0 \vec{\mathbf{W}}^{n-1}_i \\ &\quad + \frac{\Delta t}{4} \sum_{a_{ik}\in\mathcal{F}^{\text{abs}}} \int_{a_{ik}} {}^t\left(\mathbb{A}^{i\,-1}_0 \vec{\mathbf{W}}^{n-1}_i\right) \mathbb{M}_{ik} \left(\mathbb{A}^{i\,-1}_0 \left(\vec{\mathbf{W}}^{n-1}_i + \vec{\mathbf{W}}^{n+1}_i\right)\right),\end{aligned}$$

with $\mathbb{M}_{ik} = \sqrt{\mathbb{A}}^i_0 \left|\sqrt{\mathbb{A}}^{i\,-1}_0 \mathbb{P}^i_{ik} \sqrt{\mathbb{A}}^i_0\right| \sqrt{\mathbb{A}}^i_0 \equiv \sqrt{\mathbb{A}}^i_0 \left|\sqrt{\mathbb{A}}^{i\,-1}_0 \tilde{\mathbb{P}}^i_{ik} \sqrt{\mathbb{A}}^{i\,-1}_0\right| \sqrt{\mathbb{A}}^i_0$. One can show that the matrices $\mathbb{M}_{ik}$ are symmetric and positive. One can show that the variation through one time step of the aeroacoustic energy is given by:

$$\begin{aligned}\mathbb{F}^{n+1} - \mathbb{F}^n &= -\frac{\Delta t}{2} \sum_{a_{ik}\in\mathcal{F}^{\text{int}}} \int_{a_{ik}} {}^t\vec{\mathbf{V}}^n_i (\tilde{\mathbb{P}}^k_{ik} - \tilde{\mathbb{P}}^i_{ik}) \vec{\mathbf{V}}^{n+1}_k + {}^t\vec{\mathbf{V}}^{n+1}_i (\tilde{\mathbb{P}}^k_{ik} - \tilde{\mathbb{P}}^i_{ik}) \vec{\mathbf{V}}^n_k \\ &\quad - \frac{\Delta t}{4} \sum_{a_{ik}\in\mathcal{F}^{\text{abs}}} \int_{a_{ik}} {}^t\left(\vec{\mathbf{V}}^{n-1}_i + \vec{\mathbf{V}}^{n+1}_i\right) \mathbb{M}_{ik} \left(\vec{\mathbf{V}}^{n-1}_i + \vec{\mathbf{V}}^{n+1}_i\right). \qquad (10)\end{aligned}$$

where we have used the auxiliary variables $\vec{\mathbf{V}}^n_i \equiv \mathbb{A}^{i\,-1}_0 \vec{\mathbf{W}}^n_i$, $\forall i$, $\forall n$. The first term is a discrete version of the source term appearing in Eq. (6). The second term is negative and shows that our absorbing boundary conditions actually absorbs energy. This results also shows that the slip boundary condition has no influence on the global energy balance.

In order to prove stability, one can show that $\mathbb{F}^n$ is a quadratic positive definite form of numerical unknowns $(\vec{\mathbf{W}}^{n-1}_i, \vec{\mathbf{W}}^n_i)$ under some CFL-like sufficient stability condition on

the time-step Δt:

$$\forall i,\ \forall k \in \mathcal{V}_i,\ \Delta t \left(2\lambda_i \alpha_i + \beta_{ik}\rho_{ik}\right) < \frac{2V_i}{P_i}, \tag{11}$$

where α_i and β_{ik} are dimensionless regularity coefficients depending of basis functions and element aspect ratio, $\lambda_i = |u_0^i| + |v_0^i| + |w_0^i| + 3c_0^i$, and $\rho_{ik} = |\vec{v}_0^i \cdot \vec{n}_{ik}| + c_0^i$ for a boundary face and $\rho_{ik}^2 = \sup\left(\left(|\vec{v}_0^i \cdot \vec{n}_{ik}| + c_0^i\right)\right)^2 \rho\left(\mathbb{A}_0^k {\mathbb{A}_0^i}^{-1}\right), \left(|\vec{v}_0^k \cdot \vec{n}_{ik}| + c_0^k\right)^2 \rho\left(\mathbb{A}_0^i \mathbb{A}_0^{k\,-1}\right)\Big)$ for an internal face (ρ here denotes the spectral radius of a matrix).

In the case of a uniform flow, we have $\mathbb{P}_{ik}^i = \mathbb{P}_{ik}^k$. Thus the aeroacoustic energy is non-increasing (and exactly conserved if no absorbing boundary is present, which shows the scheme is genuinely non-diffusive) and the scheme is stable under a CFL-type stability condition depending on the size of elements and $\sup_i \left(\|\vec{v}_i\| + c_i^0\right)$.

3.4 Addition of a stabilization term

We have seen the energy $\mathbb{F}^n$ is not exactly conserved when the supporting flow is not uniform. However, one can show that it is indeed exactly conserved (away from absorbing boundary conditions) if a discrete source term $\mathcal{H}$ is added in each element such that:

$$\int_{\mathcal{T}_i} \mathcal{H}\vec{\varphi}_{ij} = \frac{1}{4} \sum_{k \in \mathcal{V}_i} \int_{a_{ik}} \vec{\varphi}_{ij} \cdot \left(\tilde{\mathbb{P}}_{ik}^k - \tilde{\mathbb{P}}_{ik}^i\right) \mathbb{A}_0^{k\,-1} \vec{\mathbf{W}}_k^n.$$

This property is not so intuitive, since the quadratic nature of the energy does not imply such a source term exists in general. One can notice that this source term is related to internal faces in the mesh, and that it vanishes if the flow is uniform or locally uniform. With this additional source term, the energy is conserved and therefore all numerical unknowns remain bounded.

However, one must have in mind that some instabilities should naturally occur when linearized Euler equations are considered. The addition of this source term has modified the structure of aeroacoustic equations, since Kelvin-Helmholtz instabilities for example can no more appear. Of course, one can wonder if this correction term perturbs only slightly the numerical solutions. This is tested using a 3D parallel implementation of the DGTD method (parallel MPICH Fortran 77 implementation).

4 NUMERICAL RESULTS

We dispose of a three-dimensional parallel implementation of the DGTD method presented in the previous section. Any subsonic steady flow can be considered, even with strong flow gradients. However, the flow, given as the output of a non-linear Euler equations solver, has to be post-processed: average of the flow over tetrahedra must be computed and the non-slip condition must be enforced on physical boundaries. We present in this section test-cases in two and three space dimensions, in order to validate the method on benchmark problems, test the method on complex flows and configurations,

and finally evaluate the performance of the parallel Fortran 77 implementation, based on the MPICH implementation of MPI. Parallel computations were performed on a 16 node cluster (2GHz-Pentium4 1Gb-RDRAM memory biprocessor each). In this section, tables give performance results for 64 bit arithmetic computations: N_p is the number of processes for the parallel execution, REAL denotes the total (wall clock) simulation time and CPU denotes the corresponding total CPU time taken as the maximum of the per process values. Finally, % CPU denotes the ratio of the total CPU time to the total wall clock time. This ratio clearly allows an evaluation of the CPU utilization and yields a metric for parallel efficiency.

4.1 Linear shear flow

We first consider a linearly-sheared flow ($u_0/c_0 = 0.0035y + 0.45$) for which it is well-known that no Kelvin-Helmholtz instability appears. The 200x200 computational domain is centered at the origin, with slip boundary conditions on the lower and upper boundaries, and an absorbing boundary condition on left and right boundaries. The results for a Gaussian pulse at $t = 0$ obtained for the DGTD method with ($\vec{\mathbf{W}}_{\mathcal{H}}$) or without ($\vec{\mathbf{W}}_{\mathcal{H}=0}$) the correction source term, or with Bogey's model ($\vec{\mathbf{W}}_{BBJ}$) [4] are very similar. This means that in that case the source term has no strong influence on the solution, although the influence on the discrete energy $\mathbb{F}$ is clearly visible on Figure 1 (before the pulse meets the absorbing boundary, it grows slightly for $\vec{\mathbf{W}}_{\mathcal{H}=0}$, whereas it remains constant for $\vec{\mathbf{W}}_{\mathcal{H}}$). The relative differences between $\vec{\mathbf{W}}_{\mathcal{H}}$ or $\vec{\mathbf{W}}_{BBJ}$ with $\vec{\mathbf{W}}_{\mathcal{H}=0}$ (in terms of the L^2 of the

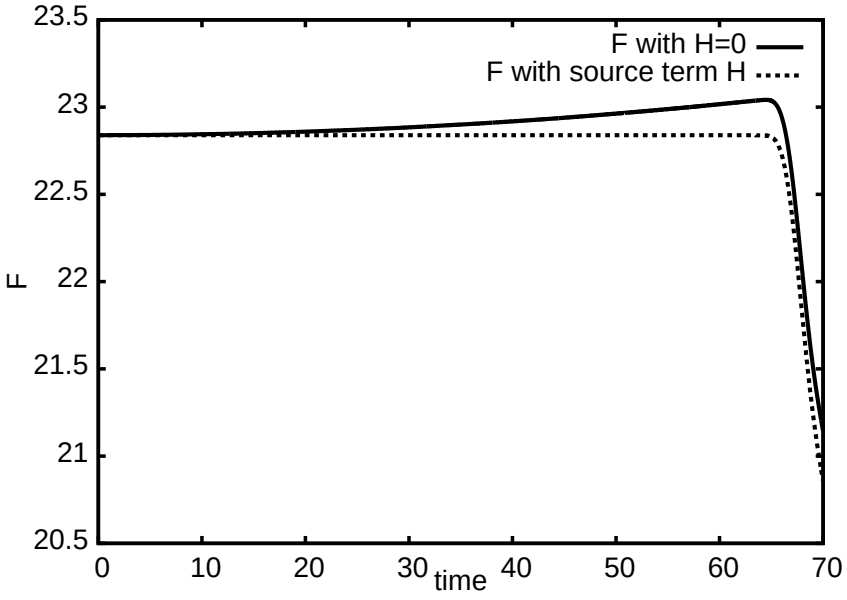

Figure 1: $\mathbb{F}$ without or with stabilization source term $\mathcal{H}$.

velocity field) are very close to each other and less than 0.1%. The results obtained with a periodic acoustic source are also almost identical (see a solution on Figure 2.

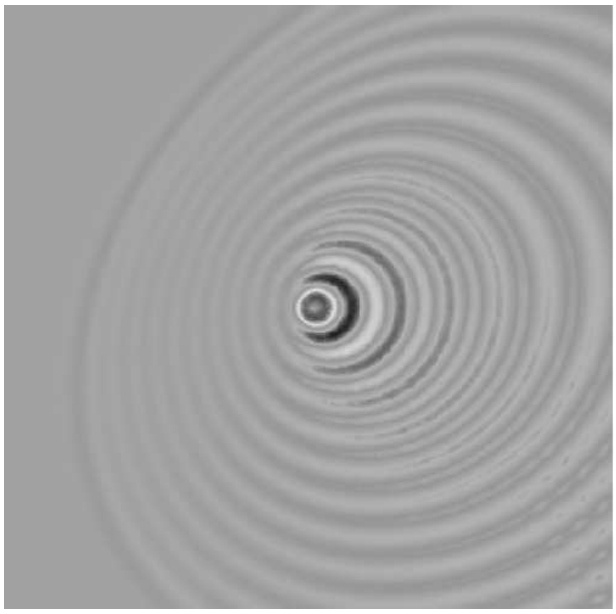

Figure 2: δp at $t = 132s$ in $\vec{\mathbf{W}}_{\mathcal{H}}$.

4.2 Unstable shear flow

We consider a similar test-case with an inflection point in the profile $u_0/c_0 = 0.5 + 0.25\tanh(151.51\ y)$, which is known to induce instabilities. A Gaussian source term at the center of the 2x0.5 domain is used. Solutions obtained with the three models are shown on Figure 3. An instability appears when no correction in the model is used, and $\vec{\mathbf{W}}_{\mathcal{H}}$ and $\vec{\mathbf{W}}_{BBJ}$ are again very similar (relative difference smaller than 0.5% in L^2 norm of the velocity field).

4.3 Aeroacoustics past a NACA profile

A steady flow with $M_\infty = 0.5$ is computed on a triangular mesh (65,580 triangles) proposed by ONERA. A time-periodic Gaussian source term is used. Instabilities were observed for this test-case for $\vec{\mathbf{W}}_{\mathcal{H}=0}$, near the leading edge. This is not the case for $\vec{\mathbf{W}}_{\mathcal{H}}$ and $\vec{\mathbf{W}}_{BBJ}$. The relative difference between these last two solutions is not far from 1%, and small differences appear near the trailing edge, where perturbations appear (see Figure 4).

4.4 Three-dimensional test-cases

We present here some computations of aeroacoustic propagation past a complex geometry. We consider the steady flow past a falcon-type geometry. The steady supporting flow was computed on a 1.31-million element tetrahedral mesh in subsonic regime ($M_\infty = 0.5$) using a 3D parallel MUSCL-based finite-volume solver [13]. The meshed surface of the aircraft along with contours for the Mach number are shown on Figure 5.

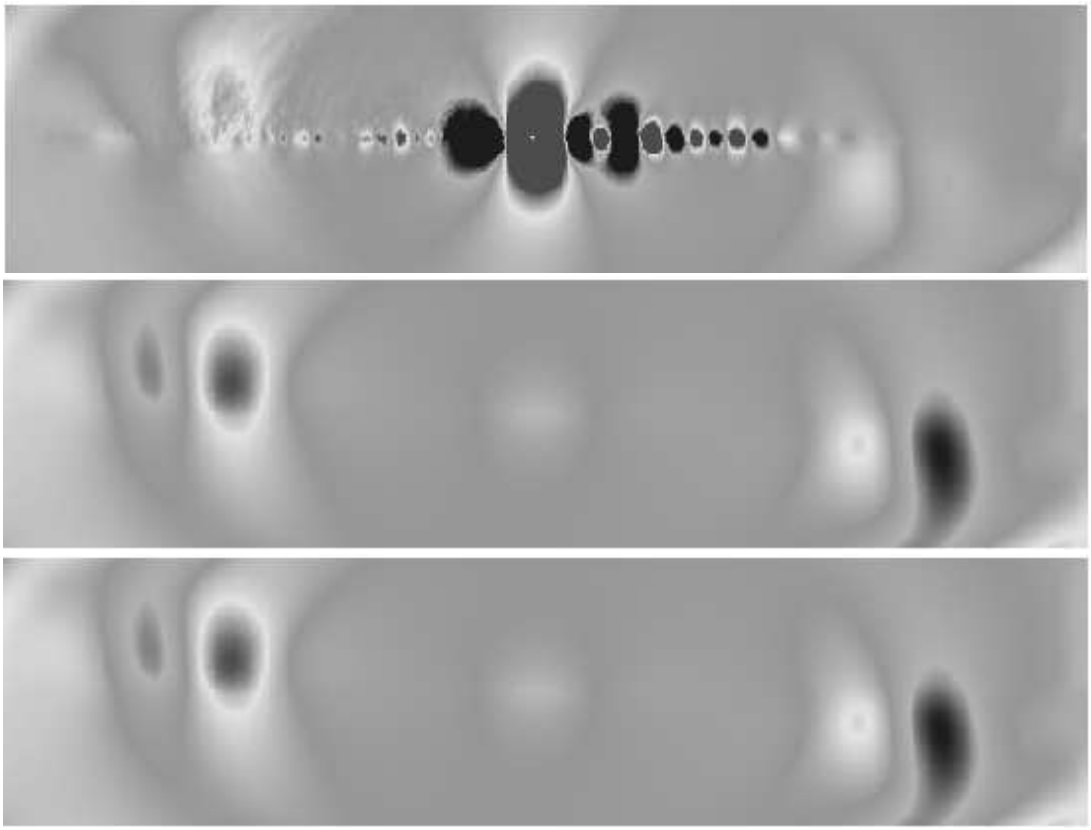

Figure 3: Contours (same scale)for δp at $t = 1s$ for $\vec{\mathbf{W}}_{\mathcal{H}=0}$ (top), $\vec{\mathbf{W}}_{\mathcal{H}}$ (middle) and $\vec{\mathbf{W}}_{BBJ}$ (bottom).

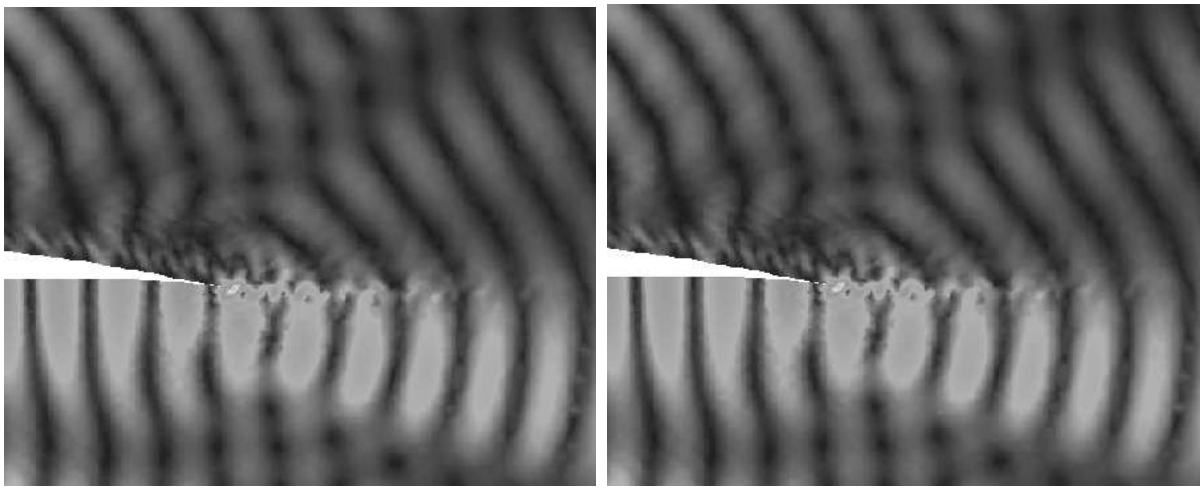

Figure 4: Zoom near the trailing edge for $\vec{\mathbf{W}}_{\mathcal{H}}$ (up) and $\vec{\mathbf{W}}_{BBJ}$ (down) with the same contours of p.

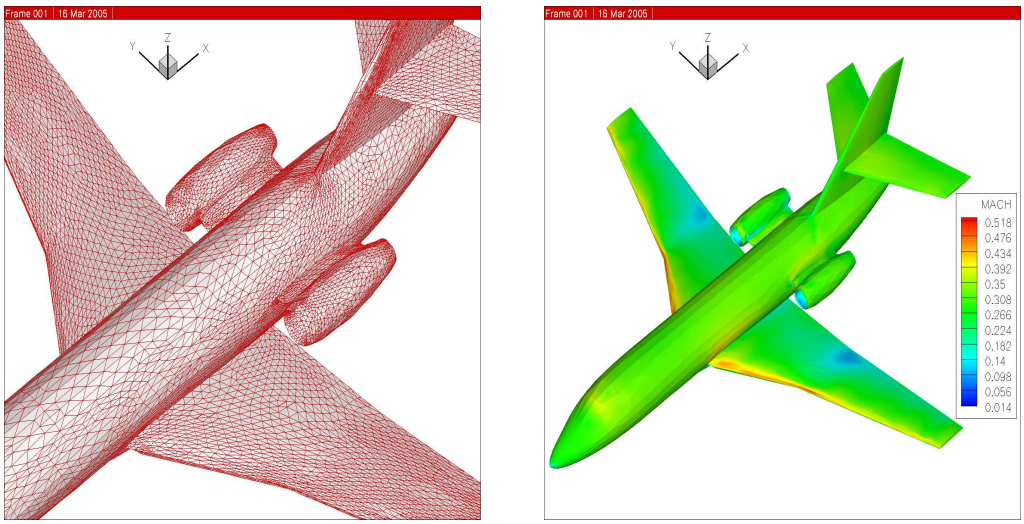

Figure 5: Meshed surface and surfacic contours of the Mach number of the supporting flow

In a first test-case, an acoustic perturbation is generated via two time-periodic Gaussian pulses (period of $T = 7ms$) located inside engines. The numerical simulation of this test-case without our stabilization revealed unstable (Tollmien-Schlichting-type instabilities). It was also unstable using the correction proposed by Bogey et al. [4]. Surface contours of $\|\delta\vec{V}\|$ at $t = 1.05s$ are shown on Figure 6 without stabilization (log-scale) and with the treatment proposed here (linear scale).

In a second test-case, an acoustic perturbation is generated via a single time-periodic Gaussian pulse (period of $T = 250ms$) located ahead of the nose of the aircraft. The stabilization was used and the computations were performed on 16 and 32 processors. Parallel efficiency and acceleration can be evaluated in Table 1. The surfacic contours of

Table 1: Aeroacoustic propagation of a perturbation : performance results

N_p	CPU time	REAL time	% CPU	$S(N_p)$
16	90h	104h	87%	1
32	52h	61h	85%	1.7

δp obtained at successive times are shown on Figure 7. The numerical results are globally in good coherence with expectations. This shows the method is able to lead to highly demanding aeroacoustic computations and that the parallel implementations is validated and quite efficient (there is room for improvement on that point). However, accuracy (measured here with the eye's norm) is acceptable but probably not high. The contours are not smooth on many parts of the surface. This could be due to the coarseness of the

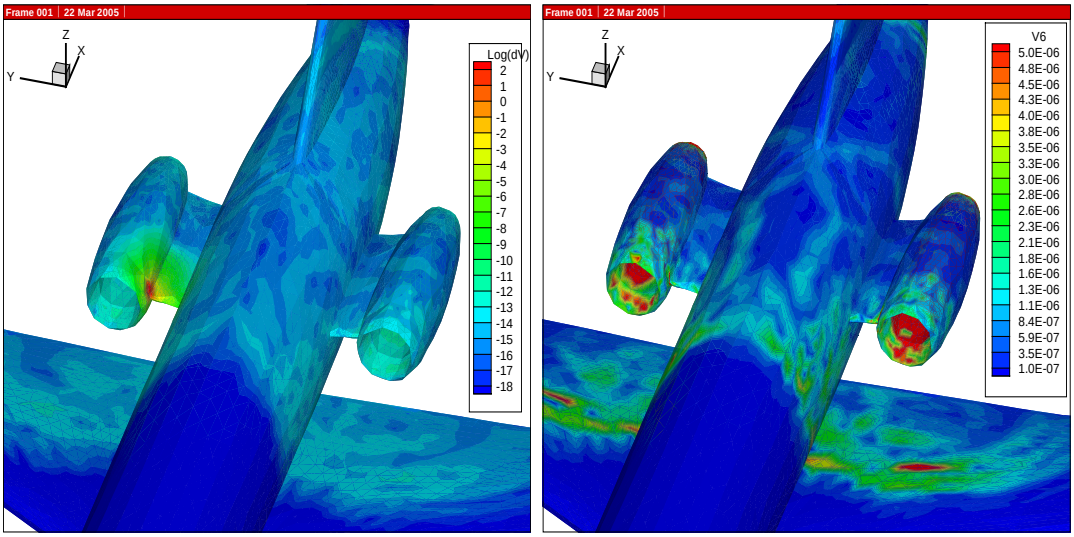

Figure 6: Surface contours of $\|\delta\vec{V}\|$ at $t = 1.05s$: without stabilization (left, log-scale) and with stabilizing source term (right, linear scale)

three-dimensional mesh used for the computations. In some regions of the supporting flow, the fact that the supporting flow is described in a finite-volume way (i.e. element-wise constant) might be responsible for such unsmoothness in the results.

5 CONCLUSION AND FURTHER WORKS

The non-dissipative DGTD framework recalled in this paper allowed for the exact control of a discrete aeroacoustic energy, including in the case of aeroacoustics in a non-uniform supporting flow. Although linearized Euler equations are not really solved, the proposition of a source term leading to the stabilization of Kelvin-Helmholtz instabilities is original and leads to interesting results.

Further works can concern many different aspects. On the modeling side, it is possible to design models for dealing with natural Kevin-Helmholtz instability, for example by adding some other source terms. This has to be done in cooperation with physicists. Anyway, the numerical framework proposed here provides a valuable tool for investigating this kind of instability in complex flows and geometries. On the numerical side, the overall accuracy could be enhanced either by considering more-than-linear basis functions ($\mathbb{P}_k$ Lagrange elements with $k > 1$) or by dealing with a more accurate description of the supporting flow (currently, it is only $\mathbb{P}_0$). Higher-order accuracy in absorbing boundary conditions and time-scheme should also be seeked for.

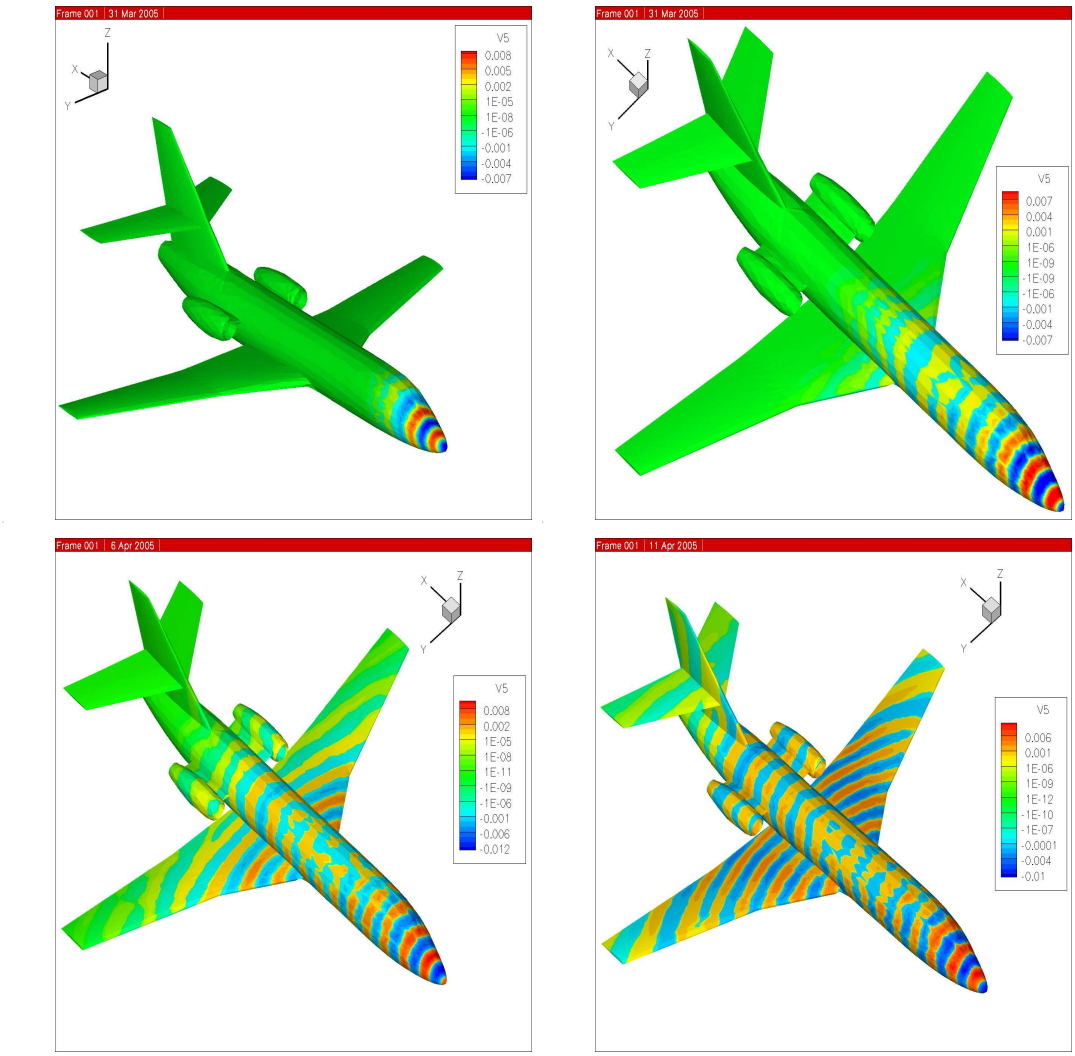

Figure 7: Surface contours for δp (times $t = 1s$, $t = 2s$, $t = 2.7$s, $t = 3.5s$).

REFERENCES

[1] S.K. Lele. Computational Aeroacoustics: a review, 35th Aerospace Sciences Meeting & Exhibit, AIAA Paper 97-0018 (1997).

[2] M. Lesieur, O. Metai., New trends in large-eddy simulations of turbulence, *Annu. Rev. Fluid Mech.*, **28**, 45–82 (1996).

[3] C.K.W. Tam and J.C. Webb. Dispersion-relation-preserving finite difference schemes for computational acoustics, *J. Comput. Phys.*, **107**, 262–281 (1993).

[4] C. Bogey, C. Bailly, D. Juvé. Computation of flow noise using source terms in linearized Euler's equations, *AIAA Journal*, **40**, 2, 235–243 (2002).

[5] C.K.W. Tam. Computational aeroacoustics: issues and methods, *AIAA Journal*, **33**, 10, 1788–1796 (1995).

[6] M.J. Lighthill. On sound generated aerodynamically-I.General theory, *Proc.Roy. Soc. London*, **211**, Ser.A, 1107, 564–587 (1952).

[7] G.M. Lilley. *The generation and radiation of supersonic jet noise*, Vol. IV - Theory of turbulence generated jet noise, noise radiation from upstream sources, and combustion noise. Part II: Generation of sound in a mixing region, Air Force Aero Propulsion Laboratory, AFAPL-TR-72-53, Vol 4, Part 2 (1972).

[8] C. Bogey, *Calcul direct du bruit aérodynamique et validation de modèles acoustiques hybrides*, Ph.D. thesis, Ecole centrale de Lyon (2000).

[9] S. Piperno and L. Fezoui. A Discontinuous Galerkin FVTD method for 3D Maxwell equations, INRIA Research Report RR-4733 (2003).

[10] A. Harten. On the symmetric form of systems of conservation laws with entropy, ICASE Research report, **81-34** (1981).

[11] J. Hesthaven and T. Warburton. Nodal high-order methods on unstructured grids. I: Time-domain solution of Maxwell's equations, *J. Comput. Phys.* **181**, 1, 186–221 (2002).

[12] M. Bernacki, S. Lanteri, and S. Piperno. Time-domain parallel simulation of heterogeneous wave propagation on unstructured grids using explicit, non-diffusive, discontinous Galerkin methods, *J. Comput. Acoust.*, **14**, 1, 57–82 (2006).

[13] S. Lanteri. Parallel solutions of compressible flows using overlapping and non-overlapping mesh patitioning strategies, *Parallel Computing*, **22**, 943–968 (1996).